Chemistry–A European Journal
Research Article
doi.org/10.1002/chem.202304050
Chemistry Europe
European Chemical Societies Publishing
www.chemeurj.org

Gold-Promoted Biocompatible Selenium Arylation of Small Molecules, Peptides and Proteins

Douglas H. Nakahata,[a] Ioannis Kanavos,[b] Maria Zubiria-Ulacia,[a, c] Alex Inague,[d] Luca Salassa,[a, c, e] Ryszard Lobinski,[b] Sayuri Miyamoto,[d] Jon Mattin Matxain,[a, c] Luisa Ronga,[b] and Raphael E. F. de Paiva*[a]

A low pKa (5.2), high polarizable volume (3.8 Å), and proneness to oxidation under ambient conditions make selenocysteine (Sec, U) a unique, natural reactive handle present in most organisms across all domains of life. Sec modification still has untapped potential for site-selective protein modification and probing. Herein we demonstrate the use of a cyclometalated gold(III) compound, [Au(bnpy)Cl_2], in the arylation of diselenides of biological significance, with a scope covering small molecule models, peptides, and proteins using a combination of multinuclear NMR (including ^{77}Se NMR), and LC–MS. Diphenyl diselenide (Ph–Se)$_2$ and selenocystine, (Sec)$_2$, were used for reaction optimization. This approach allowed us to demonstrate that an excess of diselenide (Au/Se–Se) and an increasing water percentage in the reaction media enhance both the conversion and kinetics of the C–Se coupling reaction, a combination that makes the reaction biocompatible. The C–Se coupling reaction was also shown to happen for the diselenide analogue of the cyclic peptide vasopressin ((Se–Se)-AVP), and the *Bos taurus* glutathione peroxidase (GPx1) enzyme in ammonium acetate (2 mM, pH = 7.0). The reaction mechanism, studied by DFT revealed a redox-based mechanism where the C–Se coupling is enabled by the reductive elimination of the cyclometalated Au(III) species into Au(I).

Introduction

Selenium is a vital element present in many organisms. Selenocysteine (Sec, U), the selenium analog of cysteine, is a major form of biological selenium, being considered the 21st canonical amino acid.[1] Sec is coded by the unique codon UGA, which is normally a stop codon but can be recoded to incorporate selenocysteine through the selenocysteine insertion sequence (SECIS) mechanism. The frequency of SECIS elements varies widely across the genome, but it is estimated that selenocysteine occurs in only about 25 human genes.[1] Although similar to S, Se has key chemical features that make it unique in biomolecules. Sec has a lower pK_a (5.2) than cysteine (8.3), meaning that at physiological pH, it will be present mostly as selenolate. Additionally, Se is even softer than S with a polarizable volume of 3.8 Å compared with 2.9 Å for S.[2] This combination endows Sec with an extraordinarily high nucleophilicity,[3] which is a key chemical property of Sec that distinguishes it from Cys. Sec is also easily oxidizable in ambient conditions (E° of −388 mV), resulting in selenylsulfides (Se–S) as relevant forms of biological selenium.[2,4–6] Differences in redox chemistry are also related to the fact that selenium is unable to form π bonds of any type. Therefore, while selenium reacts faster with ROS, the lack of π-bond character in the Se–O bond means that it can be more readily reduced in comparison to S-oxides.[2] Collectively this means that not all reactions exploited by Cys-targeting inhibitors can be directly translated into Sec-targeting motifs. Biologically, the properties of Sec are reflected in selenoproteins such as glutathione peroxidases (GPx) and thioredoxin reductases, which are natural antioxidants. These enzymes play key roles in the progression of many types of cancer by regulating redox signaling pathways, and by inhibiting DNA-damaging H_2O_2 and lipid peroxides.[7–9] These features make Sec a unique reactive handle, still with untapped potential for site-selective protein modifications, which has implications for cancer therapy.[4,5]

[a] Dr. D. H. Nakahata, Dr. M. Zubiria-Ulacia, Prof. L. Salassa, Prof. J. M. Matxain, Dr. R. E. F. de Paiva
Donostia International Physics Center – DIPC
Paseo Manuel de Lardizabal 4
20018 Donostia, Euskadi, Gipuzkoa, Spain
E-mail: raphael.depaiva@dipc.org
raphael.enoque@gmail.com

[b] I. Kanavos, Prof. R. Lobinski, Dr. L. Ronga
Institut des Sciences Analytiques et de Physico-Chimie Pour l'Environnement et les Matériaux – IPREM
E2S UPPA, CNRS
Université de Pau et des Pays de l'Adour
64053 Pau, France

[c] Dr. M. Zubiria-Ulacia, Prof. L. Salassa, Prof. J. M. Matxain
Polimero eta Material Aurreratuak: Fisika, Kimika eta Teknologia
Kimika Fakultatea Euskal Herriko Unibertsitatea UPV/EHU, Donostia, Spain
Euskal Herriko Unibertsitatea UPV/EHU
Paseo Manuel de Lardizabal 3
20018 Donostia, Euskadi, Gipuzkoa, Spain

[d] A. Inague, Prof. S. Miyamoto
Biochemistry Department
Institute of Chemistry
University of São Paulo
São Paulo, 05508000 SP, Brazil

[e] Prof. L. Salassa
Ikerbasque
Basque Foundation for Science
Plaza Euskadi 5
48009 Bilbao, Euskadi, Bizkaia, Spain

Supporting information for this article is available on the WWW under https://doi.org/10.1002/chem.202304050

Most metal-based tools reported in the literature for Sec chemoselective modification are based on copper systems (Figure 1).[6,10–12] Metanis *et al.*, for example, recently reported a method for Sec modification in peptides and proteins based on aryl/alkyl radicals generated from hydrazine substrates in the presence of Cu(II).[6] Despite the intrinsic affinity of gold towards selenium, this metal has been underexplored in the scope of homogenous Se arylation reactions. Spokoyny *et al.* have presented a strategy for the derivatization of nanoclusters via a gold-promoted "click"-like C–S coupling strategy. The system is based on a Me-DalPhos gold motif and the oxidative addition into aryl C–I bonds on the surface of the nanoclusters. Beyond the reactivity towards sulfur, the authors also demonstrated C–Se coupling with selenophenol in dimethylformamide in the presence of potassium phosphate.[13] In another example, Shi and colleagues presented a gold catalyst for the diselenation of alkynes and allenes, once again requiring reaction conditions that are not biocompatible.[14]

To showcase the versatility of the [Au(bnpy)Cl_2] motif (Figure 1) in chemical biology in recent years, we have recently demonstrated that [Au(bnpy)Cl_2] promotes C–S coupling with Cys residues in both a Cys_3His zinc finger domain (HIV−1 nucleocapsid, NCp7) and a Cys_2His_2 one (human transcription factor Sp1).[16] Casini and Awuah studied C–S coupling reactions with other zinc fingers and peptides.[17–19] Finally, the chemotype was explored in a glycoalbumin–Au(III) conjugate developed by Tanaka and colleagues, which enabled organ-specific labelling of proteins via lysine amidation within live mice.[20–22] The full scope of C–X coupling reactions promoted by cyclometalated Au(III) compounds has also been recently reviewed.[23–25]

Herein, we demonstrate the promising utility of [Au(bnpy)Cl_2] for the efficient arylation of small molecule diselenides and Sec-containing biomolecules, including under biocompatible conditions. The reaction was probed against diphenyl diselenide, $(Ph–Se)_2$, and selenocystine, $(Sec)_2$, chosen as small molecule aromatic and aliphatic model systems respectively. Expanding on the scope, we also demonstrate that the gold-promoted C–Se coupling reaction can also be carried out under biocompatible conditions to modify the diselenide analogue of the cyclic peptide vasopressin, (Se–Se)-AVP, and the *Bos taurus* glutathione peroxidase (GPx1) enzyme (Figure 1).

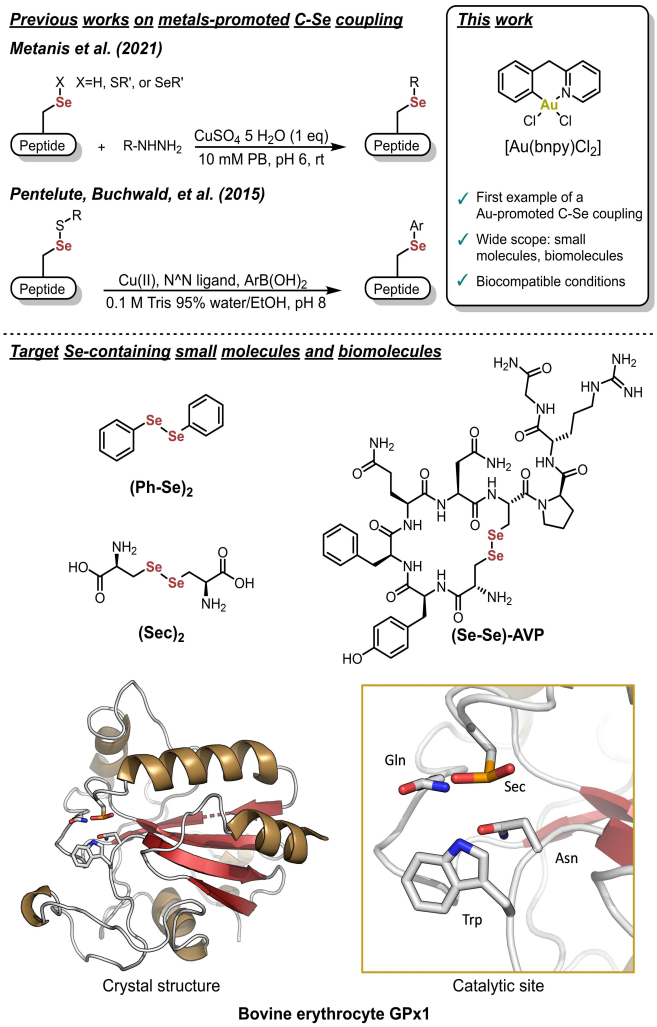

Figure 1. The cyclometalated gold(III) compound [Au(bnpy)Cl_2] is used for promoting C–Se coupling across a wide variety of substrates, including under biocompatible conditions. Previous works on metal-promoted C–Se coupling mostly explore copper.[6,11] Here, diphenyldiselenide $(Ph–Se)_2$ and selenocystine $(Sec)_2$ were selected as small molecule models. The reaction was also demonstrated with the diselenide analog of the cyclic peptide vasopressin, (Se–Se)-AVP, and the GPx1 selenoprotein from bovine erythrocytes. The GPx1 structure (PDB ID 1GP1) shown highlights the Sec-containing catalytic site (note that in the crystal structure, the Se atom is present in an oxidized state).[15]

Results and Discussion

Reaction optimization with small molecule diselenide models. Due to its high solubility in dmso and acetonitrile, $(Ph–Se)_2$ was selected as a small molecule model to probe for C–Se coupling in addition to the more biologically relevant $(Sec)_2$. The reaction of [Au(bnpy)Cl_2] with $(Ph–Se)_2$ (Figure 2a) was followed by ^{1}H NMR in dmso-d6 at different gold/diselenide stoichiometries and in the presence of increasing percentages of deuterated water in the reaction media, Figure 2b. The first set of experiments (conditions 1–4, Figure 2b) was designed to probe whether the C–Se coupling takes place, and the possible effect of the metal/diselenide stoichiometry in the coupling reaction (Figures S1–S10). The emergence of the aromatic hydrogen peak at 8.6 ppm, along with the loss of the AB pattern of the two aliphatic hydrogen atoms corresponding to the methylene group (5 and 4 ppm) are diagnostic for the formation of the Ph–Se-bnpy arylated product (Figure 2c). This observation is consistent with a freely-rotating benzyl group, implying that the ligand is not coordinated to gold(III) in a bidentate fashion upon reacting with $(Ph–Se)_2$.[16] A full assignment of the product peaks was made possible using ^{1}H–^{1}H TOCSY (Figures S16 and S17).

With [Au(bnpy)Cl_2] fixed at 5 mM, an increase in the amount of $(Ph–Se)_2$ (from 0.5 to 5 eq) only slightly increased both the conversion and the C–Se coupling rate (Figure 2d, conditions 1–4). Interestingly, a shift in the residual H_2O singlet (of dmso-d6) was observed over time whenever we had evidence of

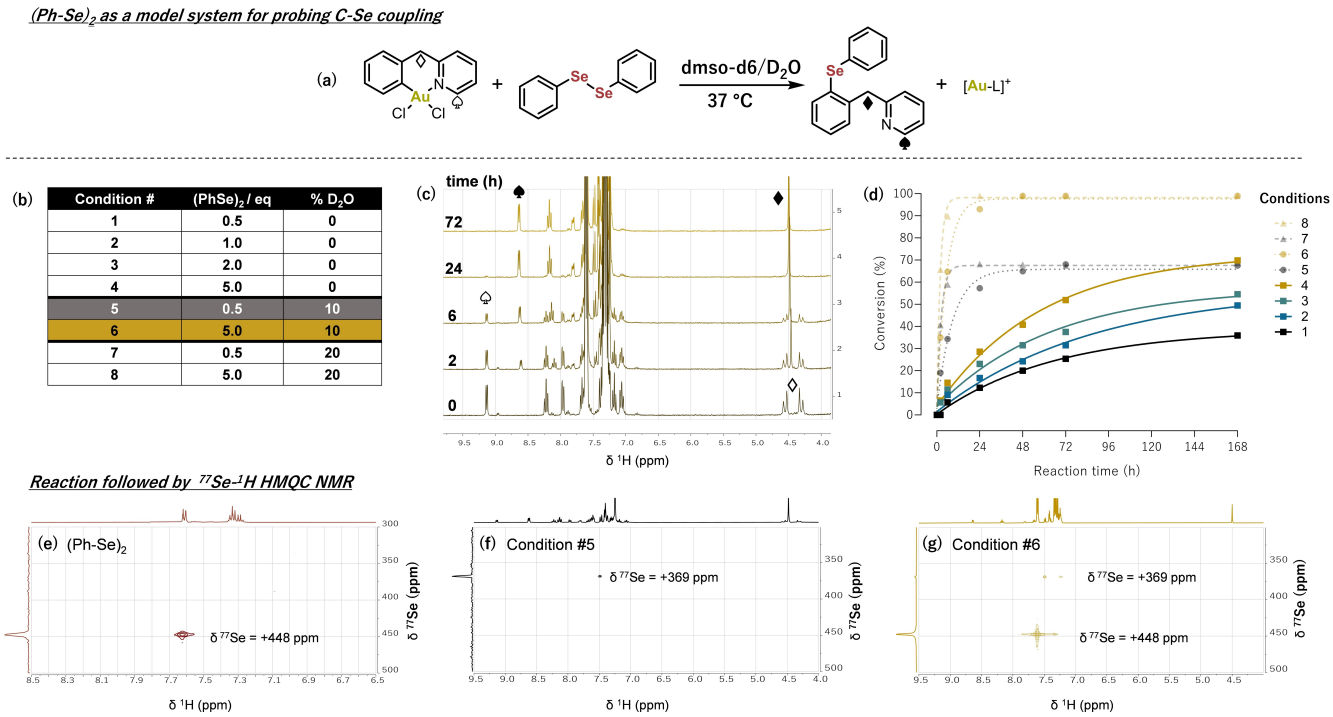

Figure 2. NMR analysis of the C–Se coupling reaction involving [Au(bnpy)Cl_2] and (Ph–Se)$_2$. **(a)** The reaction is shown in **(a)**, along with main diagnostic signals in the ^{1}H spectra annotated. **(b)** Summary of reaction conditions with [Au(bnpy)Cl_2] fixed at 5.0 mM in dmso-d6. The equivalents of (Ph–Se)$_2$ and D_2O percentage varied. **(c)** Representative time course evolution of the C–Se coupling reaction under condition 6 followed by ^{1}H NMR, with diagnostic signals annotated. **(d)** Conversion plots based on consumption of [Au(bnpy)Cl_2] (peak at 9.2 ppm) and formation of Ph–Se-bnpy (8.6 ppm). The conversion is calculated in relation to gold. **(e)** ^{77}Se-^{1}H HMQC correlation map for (Ph–Se)$_2$ 2.5 mM in dmso-d6 containing 10% D_2O. ^{77}Se-^{1}H HMQC correlation maps for reaction samples prepared following conditions 5 **(f)**, and 6 **(g)** (both incubated at 37 °C for 7 days). For the full set of NMR data of reaction conditions 1–8, control experiments and further data on the reactivity of [Au(bnpy)Cl_2] with (Ph–Se)$_2$, see Supporting Information, Figures S1–S20.

selenium arylation. This led us to hypothesize that water might play a role in the reaction mechanism. The C–Se coupling was then probed in the presence of up to 20% added D_2O in dmso-d6 (limited by the solubility of the reagents), which greatly enhanced the reaction rate and conversion (Figure 2b, conditions 5–8). As an example, using (Ph–Se)$_2$ at 25 mM in 20% D_2O led to a near complete conversion after only 6 h (Figure 2c and 2d), which confirmed that water plays an important role in the reaction mechanism (see more details below). Repeating the reaction either in acetonitrile/D_2O mixtures with varying [Au(bnpy)Cl_2]:(Ph–Se)$_2$ ratios or in neat CD_2Cl_2 led to lower conversion rates (Figures S18–S20). Consequently, a dmso/water mixture proved to be the ideal solvent system where the compounds remained soluble and the reaction proceeded with appreciable rate and conversion.

To gain a further insight into the species that emerge throughout the reaction, bidimensional ^{77}Se–^{1}H HMQC NMR measurements were performed. In dmso-d6/D_2O, the ^{77}Se signal of 2.5 mM (Ph–Se)$_2$ was observed at +448 ppm (Figure 2e). Meanwhile, the reaction product of condition 5 (cf. Figure 2b) obtained after incubation at 37 °C for 7 days appeared as a single resonance signal at +369 ppm (Figure 2f). This falls in the typical region for the ^{77}Se resonance of Ph–Se–Ph motifs,[26,27] further confirming the formation of the arylation product Ph–Se-bnpy with full consumption of (Ph–Se)$_2$. For comparison, the reaction product of condition 6, where an excess of (Ph–Se)$_2$ was present, showed both the Se-arylated product at +369 ppm and the unreacted (Ph–Se)$_2$ at +448 ppm (Figure 2g).

Liquid chromatography (LC) coupled with electrospray high resolution tandem mass spectrometry (ESI-MS/MS) gave invaluable information about the species formed throughout the reaction of (Ph–Se)$_2$ with [Au(bnpy)Cl_2] in dmso/H_2O (Figure 3). The gold(III) compound appeared as either [Au(bnpy)+formate]$^+$ or [Au(bnpy)+formate+ACN]$^+$ and the two species coeluted at t_R = 4.4 min. This can be ascribed to the sample preparation method used for LC–MS/MS, as the reaction mixtures were diluted in H_2O/ACN/formic acid. Immediate formation of the final C–Se arylation product Ph–Se-bnpy, observed as [Ph–Se-bnpy+H]$^+$ at *m/z* 326.0434 (theoretical: 326.0449) was identified for all the [Au(bnpy)Cl_2]:(Ph–Se)$_2$ ratios, albeit higher conversions were observed at higher (Ph–Se)$_2$ concentrations (in agreement with the NMR data shown in Figure 2). Finally, a third species assigned as [Ph–Se-bnpy+Au(I)]$^+$ was also observed at t = 0 h at *m/z* 522.0026 (theoretical: 522.0030) at all ratios. This species, containing a Au(I) ion, provides further experimental evidence for the reductive elimination step as part of the mechanism that leads to the C–Se coupling. LC–MS gave further evidence that the 1:0.5 [Au(bnpy)Cl_2]:(Ph–Se)$_2$ ratio was not enough to lead to full conversion even after 24 h incubation, as some unreacted cyclometalated compound is still left (in agreement with

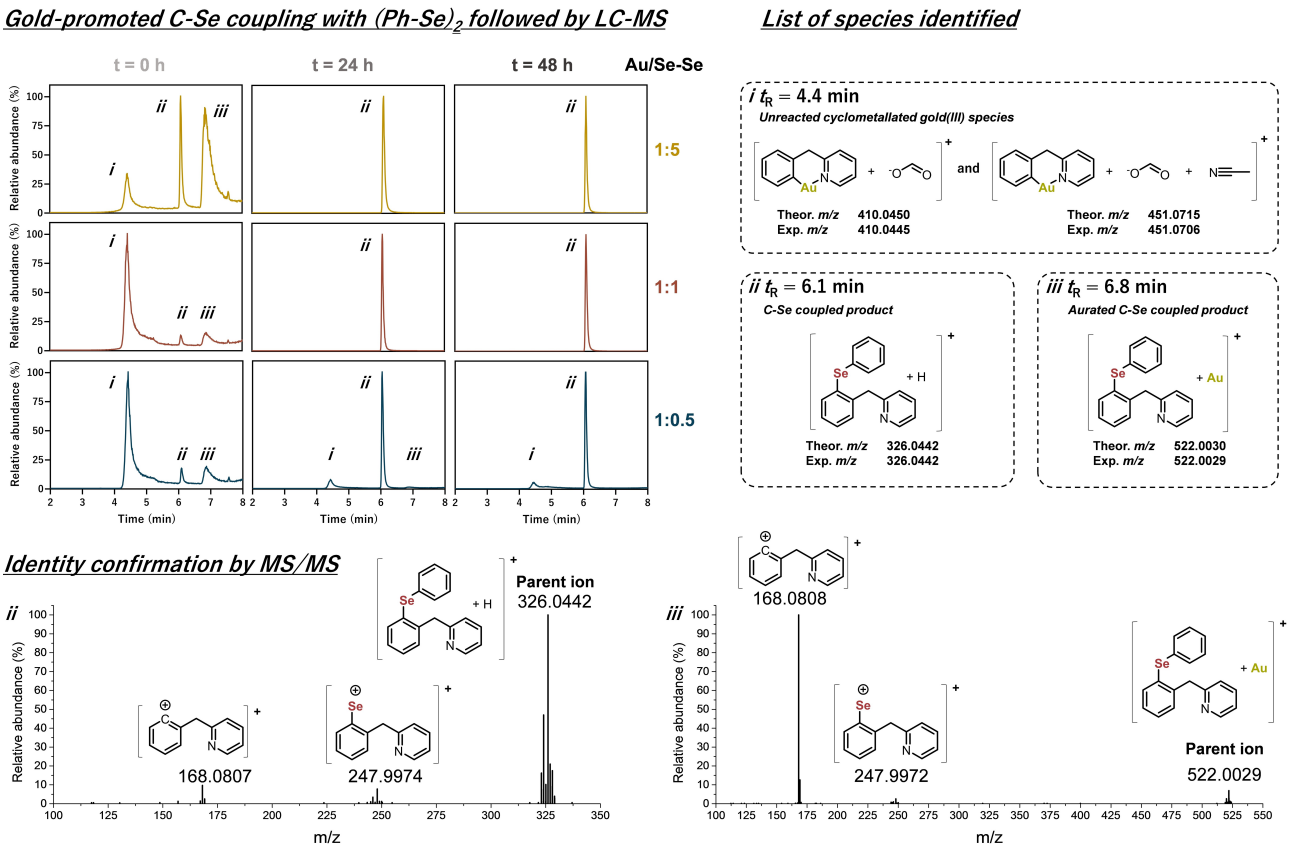

Figure 3. Au-promoted C–Se coupling reaction using $(Ph–Se)_2$ as substrate followed by LC–MS/MS. Extracted ion chromatograms (XICs) are shown for reaction mixtures prepared at varying molar ratios (1:0.5, 1:1 and 1:5) followed over time (t = 0, 24 h and 48 h). The XICs represent the relative intensity, at their characteristic m/z values, of each of the three species presented on the right-hand side, namely *i.* unreacted [Au(bnpy)] as an adduct with mobile phase components (either formate, or formate plus acetonitrile); *ii.* the final Se-arylated product; and *iii.* a Au(I) adduct with Se-arylated product. For each species, the t_R and calculated and experimental *m/z* are also given. The identity of the Se-arylated species was further confirmed by MS/MS (Higher energy Collision Dissociation, HCD = 20). The fragmentation patterns of the C–Se arylation product *ii* (*m/z* 326.0442) and the Au(I) adduct *iii* (*m/z* 522.0029) are shown at the bottom.

^{1}H NMR). Meanwhile, at either 1:1 or 1:5 ratios the Se-arylated species appeared as the only species in the chromatogram after 24 h and longer incubation times. MS/MS spectra of the *m/z* 326.0449 (Figure 3, bottom left) and the m/z 522.0029 (Figure 3, bottom right) ions confirmed the identity of these two species as the Se-arylated product $[Ph–Se\text{-}bnpy + H]^+$ and its gold(I) adduct $[Ph–Se\text{-}bnpy + Au(I)]^+$, respectively. The full LC–MS dataset, with additional ions observed throughout the experiments, is presented in Figures S21–S24.

Selenocystine, $(Sec)_2$, was studied as a biologically relevant small molecule model. This compound has the disadvantage of not being fully soluble at mM concentrations in dmso, water (at neutral pH), or their mixtures. A nominal 5 mM $(Sec)_2$ control sample in a dmso-d6/ D_2O mixture did not show any changes over 6 days (Figure S25), indicating that solvolysis of the Se–Se bond did not take place. For the reaction samples, ^{1}H NMR showed only signals assigned to the organometallic compound at t = 0 and, as the reactions progressed, a complex signal pattern arose. Taken collectively, the ^{1}H NMR data for $(Sec)_2$ (Figures S26–S30) indicated the presence of three distinct species, present in equilibrium after 7 days of reaction: unreacted $[Au(bnpy)Cl_2]$, [Sec-bnpy + Au(I) + Cl^-], and the arylated product Sec-bnpy (this assignment is also consistent with LC–MS data; see below). The presence of each species varied depending on the Se/Au stoichiometric ratio and the percentage of water in the reaction medium. Further evidence for the Sec-bnpy product was obtained by recording the ^{77}Se–^{1}H HMQC spectra of reaction mixtures containing 1:5 $[Au(bnpy)Cl_2]$:$(Sec)_2$ in the presence of either 10 and 20% D_2O (Figure S31). In both cases, a signal at +215 ppm was observed, which falls is in the range of $Ph–Se\text{-}CH_3$ species.[26,27] LC–MS studies (Figures S32–S35) revealed that the main species present in the reaction mixtures was Sec-bnpy in an adduct with gold(I) (*m/z* 533.0021), which was further confirmed by MS/MS.

Although equivalent species appear throughout the reaction of $[Au(bnpy)Cl_2]$ with both $(Ph–Se)_2$ and $(Sec)_2$, it is relevant to highlight a key difference. In the case of $(Ph–Se)_2$, the main product is the Se-arylated species (Figure 3, species *ii*) while in the case of $(Sec)_2$, the main product is the Se-arylated adduct with gold(I) (Figure S32, species *iii*). This can be related to the higher basicity of the selenium atom in the Sec-containing aliphatic product as opposed to the aromatic product formed with $(Ph–Se)_2$.

Since $(Sec)_2$ has limited solubility at neutral pH, we also investigated the reactivity of $[Au(bnpy)Cl_2]$ with $(Sec)_2$ fully dissolved in dmso-d6 with added 40 mM DCl (Figure S36). Evidence of arylation was also observed under this experimental condition, but appreciable conversions were detected only after long incubation times. Interestingly, a species at *m/z* 735.9323 (Figure S37 to S40) was identified as $[Au(bnpy)Cl+(Sec)_2]^+$, which indicated direct coordination of the intact diselenide species to the cyclometalated gold(III). This observation sheds light on the very first step of reaction mechanism. After 24 h of incubation at 37 °C, the major species was again the aurated Sec-bnpy species.

C–Se coupling in selenopeptides and selenoproteins. Next, expanding on the scope of the Se-arylation reaction, we demonstrate further that $[Au(bnpy)Cl_2]$ can promote C–Se coupling in a model selenopeptide sequence, (Se–Se)-AVP, and in a full selenoprotein, the GPx1 from *Bos taurus* erythrocytes (both shown in Figure 1). The Se isotope pattern is a diagnostic feature that was exploited across all these experiments to confirm the arylation on Sec.

The selenopeptide model (Se–Se)-AVP is the diselenide analogue of the hormone vasopressin (AVP), which is a nonapeptide hormone best known for its antidiuretic and vasopressor actions.[28] The synthesis of (Se–Se)-AVP was described elsewhere,[29,30] and it has been proposed as a model for studying the reactivity of metal complexes and metal ions of medical and environmental relevance.[31–33] The reaction was studied either at 1:5 $[Au(bnpy)Cl_2]$ to (Se–Se)-AVP in water/dmso (40/60) (Figure S41) or 1:1 in 2 mM NH_4OAc (Figure S42). In both cases, two gold-containing species were identified (peak *b* and *c*, Figures S41 and S42). The main product *c* (peak at $t_R = 4.35$ min) corresponds to a single species of *m/z* 732.22. This modified peptide contains one selenium atom as evidenced by the isotope pattern and one gold atom. The MS/MS data (Figure 4) provided further structural information, revealing the deselenization of Sec6 into dehydroalanine and

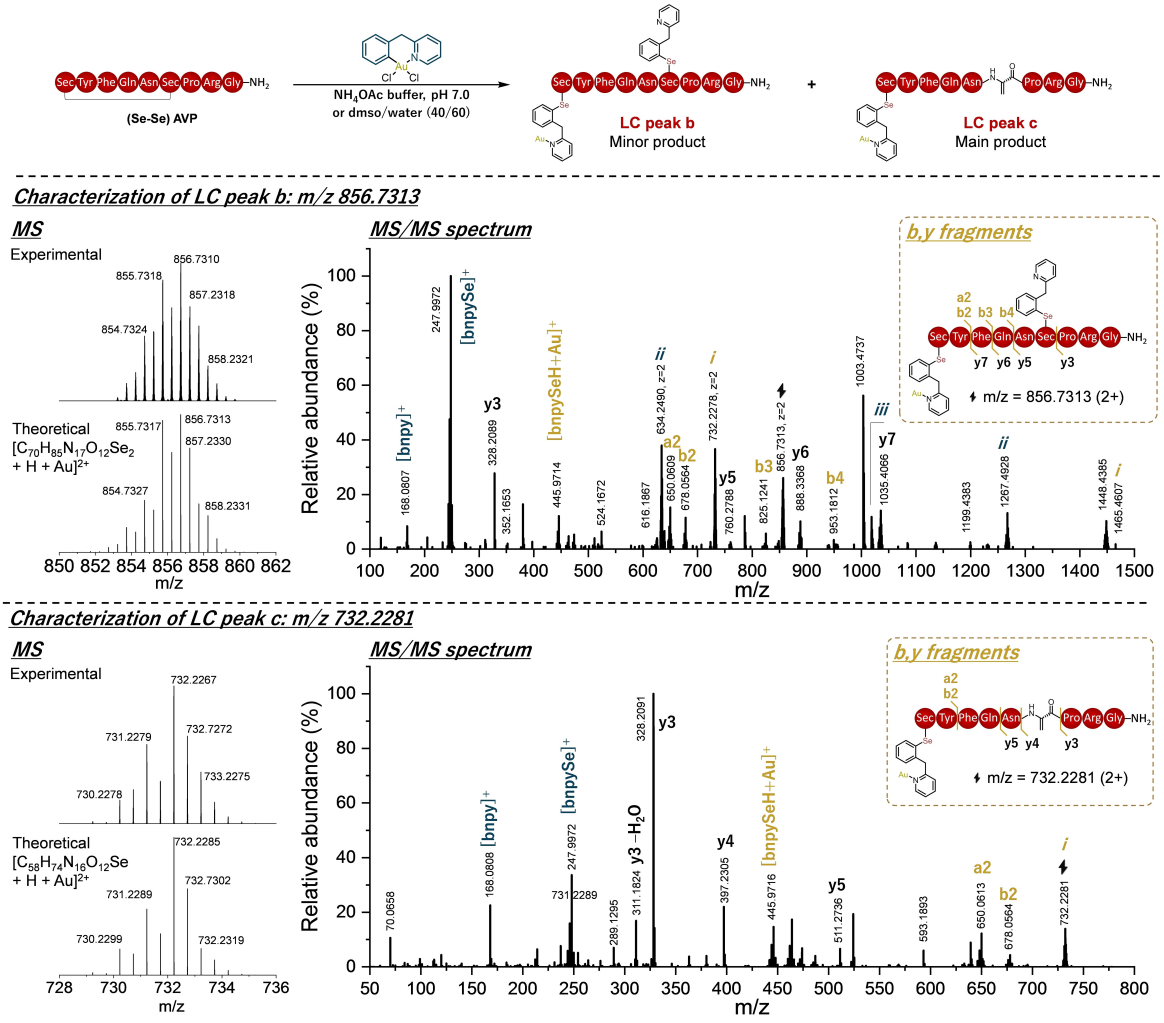

Figure 4. MS/MS spectra of representative species that provide evidence for the arylation of (Se–Se)-AVP (1:1 or 1:5 gold/peptide and in either dmso/water (40/60) or in 2 mM NH_4OAc, pH = 7.0). The peak at *m/z* 732.22 is the main reaction product observed across all conditions (see Figures S41 and S42), while the peak at *m/z* 856.7313 corresponds to the gold(I) adduct of the bisarylated peptide. The experimental and theoretical isotope patterns of each ion is given on the left hand side of the figure. Both species were subjected to MS/MS (HCD 20), further confirming the identity of the arylated positions within the peptide sequence, and the position of the gold atom along the sequence. The b and y fragments were assigned, while fragments denoted in roman numerals dehydroalanine, which arises *via* β-elimination. Gold-containing fragments are marked in golden characters.

the arylation of Sec1. Additionally, the modified Sec1 appears as an adduct with gold(I) as evidenced by fragments a2 and b2. Deselenization of Sec into dehydroalanine *via* β-elimination is a well reported mechanism.[34,35] On the other hand, the less abundant product b contains a species at *m/z* 856.73 with two selenium atoms (isotope pattern shown in Figure 4), along with one gold atom. The MS/MS spectrum (Figure 4) revealed the arylation of both Sec residues. Additionally, the modified Sec 1 residue appeared as an adduct with Au(I) as evidenced by fragments a2, b2, b3 and b4. A list of all dehydroalanine-containing fragments identified by MS/MS of the *m/z* 856.73 ion is shown in Figure S43. Mechanistically, the fact that the species at *m/z* 732.2285 corresponds to the main reaction product demonstrates that deselenization itself is either related to or even promoted by the Se-arylation reaction, and not merely an HCD artefact.

Among other studied gold compounds, auranofin and related gold(I) phosphine complexes were shown to promote Sec metalation in (Se–Se)-AVP, although that happens only when either the peptide had been previously treated with a reducing agent (*i.e.* dithiothreitol) or when the reaction had been carried out at 70 °C.[31,32]

Contrasting to its reactivity with (Se–Se)-AVP, when [Au(bnpy)Cl_2] was incubated with its disulfide analog AVP (1 : 5) in water/dmso (40/60), very small amounts of any arylated product could be detected even after 6 days (Figure S44). This gives initial evidence of selectivity of the cyclometallated [Au(bnpy)Cl_2] towards Sec in relation to Cys.

Finally, incubation of [Au(bnpy)Cl_2] with GPx1 from *Bos taurus* erythrocytes[36] (> 90 % BLAST[37] sequence identity with the human GPx1 homologue) at two distinct ratios under biocompatible conditions (2 mM NH_4OAc, pH = 7.0) showed a clear evolution in the number of arylation sites over time (Figure 5).

Deconvoluted MS provided evidence of adduct formation with 2 bnpy ligands at t = 0. The presence of protein species containing more bnpy modifications than gold (*i.e.* 2 Au, 3 bnpy; 3 Au, 4 bnpy; 3 Au, 5 bnpy; 4 Au, 5 bnpy; Figure 5) is strong evidence for arylation, rather than just coordination of the cyclometalated [Au(bnpy)]$^{n+}$ motif to the protein. For the reaction at a 5 : 1 gold/protein ratio, up to 5 gold ions and 6 bnpy groups were incorporated, which indicated that a total of 6 protein sites have been arylated under these conditions. We and others have demonstrated that [Au(bnpy)Cl_2] has excellent chemoselectivity towards Cys, with no cross-reactivity with side-chains that contain either free amines or carboxylates for example.[16,18,38] The GPx1 enzyme from bovine erythrocytes has 1 Sec and 5 Cys residues[36], which can therefore be proposed as the arylated sites. The raw MS data for the unreacted GPx1 protein and the reaction products are given in Figures S45–S48.

Thioredoxin reductase has been the usual target selenoprotein for gold compounds.[39,40] While many authors have reported the potential inhibitory effect of gold compounds on this enzyme, only a few studies focused on the identification of the metal binding sites.[40,41] A recent preprint described the use of a modified benzoylpyridine ligand cyclometalated with gold(III) for identifying interactors in SW480 cell lysates via

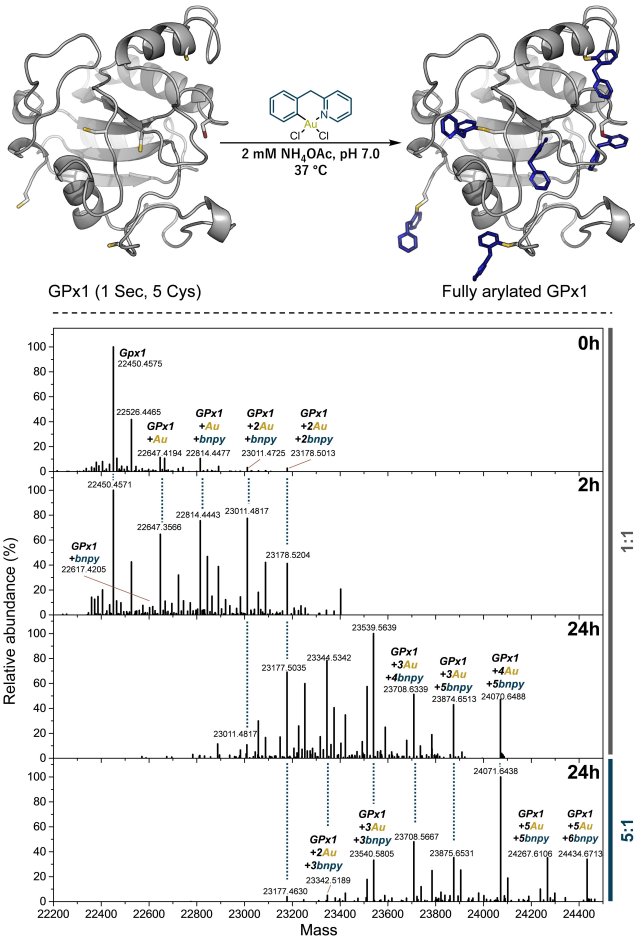

Figure 5. Top: Reaction of GPx1 from *Bos taurus* erythrocytes with [Au(bnpy)Cl_2] under biocompatible conditions (2 mM NH_4OAc in water, pH 7.0, 37 °C). The Sec residue and the 5 Cys residues were assigned as the arylation sites. The bnpy ligand, transferred to the protein upon C–Se and C–S bond formation, are marked in blue. Bottom: The reaction was followed over time and the deconvoluted MS are shown for reaction mixtures at either 1 : 1 or 5 : 1 [Au(bnpy)Cl_2] : GPx1 ratio. Each peak was assigned based on the number of arylated sites and gold atoms present in the adduct.

chemoproteomic approaches. Thioredoxin reductase 1 (TXNRD1) was observed as the major interactor, via a double arylation at the C-terminal CysSec dyad.[42]

For glutathione peroxidases, there are scarce reports indicating that gold(I)[40,43–45] and gold(III)[46] compounds act as their inhibitors. Specifically, recent findings indicated that auranofin functions as an inhibitor of GPx1; however, it did not exert significant inhibitory effects on GPx4.[47] To the best of our knowledge, no other studies had explored the molecular basis of the inhibition of this family of selenoproteins by gold compounds.

C–Se coupling mechanism investigated by DFT. DFT calculations were used to support the mechanism of the gold-promoted C–Se coupling reaction. Figure 6 shows the mechanism proposed for both the aliphatic *N*-acetyl selenocysteinate (in black), which serves as a model for Sec incorporated into peptides and proteins under physiological pH (anionic form). The aromatic phenylselenide was also considered (in gray), for comparison purposes. Geometry optimization and vibrational

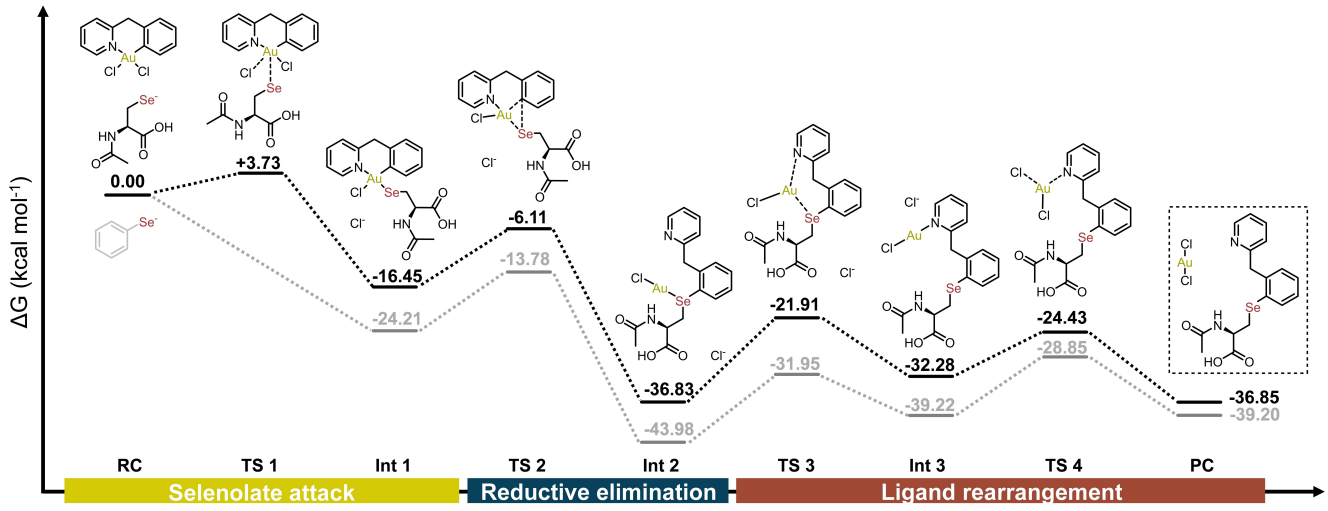

Figure 6. Full Gibbs free energy surface for the Au-promoted C–Se coupling reaction mechanism proposed by DFT at the M06/6-311++G(2df,2p) level of theory for non-metal atoms and ECP60MDF/aug-cc-pVDZ-PP for Au. Only the species involving *N*-acetyl selenocysteinate are fully represented (reaction pathway shown in black), while the species and corresponding energies for phenylselenide are shown in gray. In each system, there is a total of 9 explicit water molecules that are not shown in this simplified diagram for the sake of clarity. For the full structures of each species including explicit water molecules please refer to the supplementary information (**RC** = reactant complex; **TS** = transition states; **Int** = intermediates; **PC** = product complex). The reaction coordinate is split in three phases: the attack of the selenolate to the cyclometalated gold(III) compound and incorporation cis to the C-donor; the reductive elimination step, enabling the C–Se coupling; and a ligand rearrangement that allows the release of the gold(I) species.

frequencies were carried out by DFT at the M06/6-31+G(d,p) level of theory for non-metal atoms and ECP60MDF / aug-cc-pVDZ-PP for Au.

The attack of the selenolate to $[Au(bnpy)Cl_2]$ followed by its incorporation *cis* to the C-donor is energetically favorable for both the selenocysteinate and phenylselenolate (Figure S49). Moreover, if the incorporation is *cis* to the N-donor, the reaction is unproductive as expected. These steps are grouped in yellow in Figure 6. Afterwards, the reaction proceeds *via* reductive elimination, which enables the C–Se coupling (Int 2, overcoming TS 2) to take place. The final dissociation of Au(I) from the C–Se coupled product requires two nucleophilic attacks, first by the pyridine of the benzylpyridine motif which then facilitates the attack of a chloride leading to $[AuCl_2]^-$ and dissociation of the C–Se coupled product. Both Int 2 where gold(I) is coordinated to the selenoether, or Int 3, where gold(I) coordinated to the pyridine motif, provide theoretical support for the ubiquitous species that was identified by MS for both $(Ph–Se)_2$ (Figure 3, species *iii*, *m/z* 522.0029), and $(SeCys)_2$ (Figure S32, *m/z* 533.0030).

The mechanism proposed here for the gold-promoted C–Se coupling, where reductive elimination enables the cross-coupling,[48,49] is similar to those previously reported for C–S,[17,50] C–C,[51] and C–P[52] coupling reactions. A previously reported DFT mechanism demonstrated that the bis substitution of the chlorido ligands in the [Au(bnopy)Cl2] and related motifs (bnopy = 2-benzoylpyridine–H) by cysteinates was advantageous for the C-S coupling reaction progression.[17,18] Here for the C–Se coupling we do observe experimentally a reaction rate increase when an excess of diselenide is present (e.g., 5:1 diselenide to gold as shown in Figure 2b and 2c), but the reaction still happens with appreciable conversions when the cyclometalated gold(III) compound is exposed to stoichiometric amounts of selenium. This information was used as basis for our DFT-proposed mechanism. Additionally, DFT demonstrated that the presence of explicit water molecules was critical to stabilize charged species throughout the reaction. The supporting information section 3.13 gives the full coordinates for each species mentioned in Figure 6, including the position of explicit water molecules. This observation lends theoretical support for the role played by water in the C–Se coupling reaction asobserved experimentally by NMR.

Conclusions

Our investigation adds organometallic gold(III) compounds to the still scarce toolkit of metal-based systems apt at facilitating selenium arylation. This contribution broadens the horizons accessible to synthetic and medicinal chemists, affording a new tool for the construction of selenium-containing organic molecules, which are promising chemotypes in drug design. $[Au(bnpy)Cl_2]$ was able to promote arylation of $(Sec)_2$ and $(Ph–Se)_2$, including under biocompatible conditions, with water itself playing a role in the reaction progression (rate and conversion). The arylation of (Se–Se)-AVP took place at both Sec residues, and we have strong evidence that arylated Sec residues can also undergo deselenization into dehydroalanine. Meanwhile, the reaction of $[Au(bnpy)Cl_2]$ with AVP did not lead to appreciable amounts of the arylated product, indicating chemoselectivity towards Se–Se over S–S. In the case of GPx1, full arylation of the protein was observed across the Sec residue and the 5 Cys residues. With the promising results reported here towards Se arylation, further structural changes around the bnpy motif are under investigation. DFT mechanistic analysis has shed light on the reductive elimination and ligand

rearrangement as critical steps for C–Se coupling in water, paving the way for further structural variation of the [Au(bnpy)Cl_2] motif for enhanced selectivity and efficiency in Au-mediated arylation reactions. Additionally, the biocompatibility of the reaction opens a new avenue towards exploring *in situ* intracellular selenoprotein modification and selenoenzyme inhibition.

Supporting Information

The authors have cited additional references within the Supporting Information.[53–61]

Acknowledgements

This project has received funding from "la Caixa" Foundation (ID 100010434) through the Junior Leader fellowship to RdP (LCF/BQ/PI22/11910033). The São Paulo Research Foundation (FAPESP; www.fapesp.br) is acknowledged – grants CEPID-Redoxoma 2013/07937-8 to SM and fellowship 2017/13804-1 to AI. The authors thank Dr. José Ignacio Miranda (UPV/EHU, SGIker) for the aid and fruitful discussions with the ^{77}Se NMR measurements. Technical and human support provided by SGIker (UPV/EHU, MICINN, GV/EJ, ERDF and ESF) is also acknowledged. The Donostia International Physics Center receives support from the "Severo Ochoa" Program for Centers of Excellence in R&D (Grants CEX2018-000867-S) run by the Spanish State Research Agency. This research has also received Funding from the European Union's Horizon H2020 Research and Innovation under the Marie Skłodowska-Curie Grant Agreement N° 945416 through the PhD fellowship of IK. The authors thank Dr. Simon Godin for training and technical assistance with LC–MS/MS apparatus, and C. Enjalbal and E. Cordeau for providing the synthetic (Se–Se)-AVP peptide.

Conflict of Interests

The authors declare no conflict of interest.

Data Availability Statement

The data that support the findings of this study are available in the supplementary material of this article.

Keywords: arylation · diselenides · selenocysteine, selenopeptides, and selenoproteins · cyclometalated gold compounds · biocompatible reactions

[1] R. L. Schmidt, M. Simonović, *Croat Med J* **2012**, *53*, 535–550.
[2] H. J. Reich, R. J. Hondal, *ACS Chem. Biol.* **2016**, *11*, 821–841.
[3] E. S. J. Arnér, *Exp. Cell Res.* **2010**, *316*, 1296–1303.
[4] C. Zhang, E. V. Vinogradova, A. M. Spokoyny, S. L. Buchwald, B. L. Pentelute, *Angew. Chem. Int. Ed.* **2019**, *58*, 4810–4839.
[5] R. Mousa, R. Notis Dardashti, N. Metanis, *Angew. Chem. Int. Ed.* **2017**, *56*, 15818–15827.
[6] Z. Zhao, D. Shimon, N. Metanis, *J. Am. Chem. Soc.* **2021**, *143*, 12817–12824.
[7] D. L. Hatfield, P. A. Tsuji, B. A. Carlson, V. N. Gladyshev, *Trends Biochem. Sci.* **2014**, *39*, 112–120.
[8] S. P. Short, C. S. Williams, in *Advances in Cancer Research* (Eds.: K. D. Tew, F. Galli), Academic Press, **2017**, pp. 49–83.
[9] W. Wu, D. Li, X. Feng, F. Zhao, C. Li, S. Zheng, J. Lyu, *BMC Medical Genomics* **2021**, *14*, 78.
[10] P. Arsenyan, S. Lapcinska, A. Ivanova, J. Vasiljeva, *Eur. J. Org. Chem.* **2019**, *2019*, 4951–4961.
[11] D. T. Cohen, C. Zhang, B. L. Pentelute, S. L. Buchwald, *J. Am. Chem. Soc.* **2015**, *137*, 9784–9787.
[12] I. P. Beletskaya, V. P. Ananikov, *Chem. Rev.* **2022**, *122*, 16110–16293.
[13] J. M. Stauber, E. A. Qian, Y. Han, A. L. Rheingold, P. Král, D. Fujita, A. M. Spokoyny, *J. Am. Chem. Soc.* **2020**, *142*, 327–334.
[14] J. Wang, C. Wei, X. Li, P. Zhao, C. Shan, L. Wojtas, H. Chen, X. Shi, *Chem. Eur. J.* **2020**, *26*, 5946–5950.
[15] O. Epp, R. Ladenstein, A. Wendel, *Eur. J. Biochem.* **1983**, *133*, 51–69.
[16] R. E. F. De Paiva, Z. Du, D. H. Nakahata, F. A. Lima, P. P. Corbi, N. P. Farrell, *Angew. Chem. Int. Ed.* **2018**, *57*, 9305–9309.
[17] M. N. Wenzel, R. Bonsignore, S. R. Thomas, D. Bourissou, G. Barone, A. Casini, *Chem. Eur. J.* **2019**, *25*, 7628–7634.
[18] S. R. Thomas, R. Bonsignore, J. Sánchez Escudero, S. M. Meier-Menches, C. M. Brown, M. O. Wolf, G. Barone, L. Y. P. Luk, A. Casini, *ChemBioChem* **2020**, *21*, 3071–3076.
[19] S. Gukathasan, S. Parkin, E. P. Black, S. G. Awuah, *Inorg. Chem.* **2021**, *60*, 14582–14593.
[20] K. Tsubokura, K. K. H. Vong, A. R. Pradipta, A. Ogura, S. Urano, T. Tahara, S. Nozaki, H. Onoe, Y. Nakao, R. Sibgatullina, A. Kurbangalieva, Y. Watanabe, K. Tanaka, *Angew. Chem. Int. Ed.* **2017**, *56*, 3579–3584.
[21] Y. Lin, K. Vong, K. Matsuoka, K. Tanaka, *Chem. - Eur. J.* **2018**, *24*, 10595–10600.
[22] P. Ahmadi, K. Muguruma, T.-C. Chang, S. Tamura, K. Tsubokura, Y. Egawa, T. Suzuki, N. Dohmae, Y. Nakao, K. Tanaka, *Chem. Sci.* **2021**, *12*, 12266–12273.
[23] L. Rocchigiani, M. Bochmann, *Chem. Rev.* **2021**, *121*, 8364–8451.
[24] G. Moreno-Alcántar, P. Picchetti, A. Casini, *Angewandte Chemie International Edition* **2023**, *n/a*, e202218000.
[25] R. T. Mertens, S. Gukathasan, A. S. Arojojoye, C. Olelewe, S. G. Awuah, *Chem. Rev.* **2023**, DOI: 10.1021/acs.chemrev.2c00649.
[26] H. Duddeck, in *Chemical Shifts and Coupling Constants for Selenium-77* (Eds.: R. R. Gupta, M. D. Lechner), Springer-Verlag, Berlin/Heidelberg, **2004**, pp. 1–11.
[27] M. S. Silva, D. Alves, D. Hartwig, R. G. Jacob, G. Perin, E. J. Lenardão, *Asian J. Org. Chem.* **2021**, *10*, 91–128.
[28] M. Yoshimura, B. Conway-Campbell, Y. Ueta, *Peptides* **2021**, *142*, 170555.
[29] E. Cordeau, C. Arnaudguilhem, B. Bouyssiere, A. Hagège, J. Martinez, G. Subra, S. Cantel, C. Enjalbal, *PLoS One* **2016**, *11*, e0157943.
[30] M. Mobli, D. Morgenstern, G. F. King, P. F. Alewood, M. Muttenthaler, *Angew. Chem. Int. Ed.* **2011**, *50*, 11952–11955.
[31] J. Lamarche, E. A. Álvarez, E. Cordeau, C. Enjalbal, L. Massai, L. Messori, R. Lobinski, L. Ronga, *Dalton Trans.* **2021**, *50*, 17487–17490.
[32] L. Ronga, I. Tolbatov, E. Giorgi, P. Pisarek, C. Enjalbal, A. Marrone, D. Tesauro, R. Lobinski, T. Marzo, D. Cirri, A. Pratesi, *Inorg. Chem.* **2023**, *62*, 10389–10396.
[33] M. Bernabeu De Maria, D. Tesauro, F. Prencipe, M. Saviano, L. Messori, C. Enjalbal, R. Lobinski, L. Ronga, *Inorg. Chem.* **2023**, acs.inorgchem.3c01708.
[34] R. Quaderer, D. Hilvert, *Chem. Commun.* **2002**, 2620–2621.
[35] S. Ma, R. M. Caprioli, K. E. Hill, R. F. Burk, *J. Am. Soc. Mass Spectrom.* **2003**, *14*, 593–600.
[36] P. Gettins, D. Dyal, B. Crews, *Arch. Biochem. Biophys.* **1992**, *294*, 511–518.
[37] M. Johnson, I. Zaretskaya, Y. Raytselis, Y. Merezhuk, S. McGinnis, T. L. Madden, *Nucleic Acids Res.* **2008**, *36*, W5–W9.
[38] K. K.-Y. Kung, H.-M. Ko, J.-F. Cui, H.-C. Chong, Y.-C. Leung, M.-K. Wong, *Chem. Commun.* **2014**, *50*, 11899–11902.
[39] A. Bindoli, M. P. Rigobello, G. Scutari, C. Gabbiani, A. Casini, L. Messori, *Coord. Chem. Rev.* **2009**, *253*, 1692–1707.
[40] M. Bernabeu de Maria, J. Lamarche, L. Ronga, L. Messori, J. Szpunar, R. Lobinski, *Coord. Chem. Rev.* **2023**, *474*, 214836.
[41] I. J. Pickering, Q. Cheng, E. M. Rengifo, S. Nehzati, N. V. Dolgova, T. Kroll, D. Sokaras, G. N. George, E. S. J. Arnér, *Inorg. Chem.* **2020**, *59*, 2711–2718.

[42] L. Skos, C. Schmidt, S. Thomas, M. Park, R. Bonsignore, G. Del Favero, T. Mohr, A. Bileck, C. Gerner, A. Casini, S. M. Meier-Menches, *ChemRxiv*. **2023**, DOI: 10.26434/chemrxiv-2023-plbdr.
[43] V. Gandin, A. P. Fernandes, M. P. Rigobello, B. Dani, F. Sorrentino, F. Tisato, M. Björnstedt, A. Bindoli, A. Sturaro, R. Rella, C. Marzano, *Biochem. Pharmacol.* **2010**, *79*, 90–101.
[44] J. R. Roberts, C. F. Shaw, *Biochem. Pharmacol.* **1998**, *55*, 1291–1299.
[45] M. A. Baker, A. L. Tappel, *Biochem. Pharmacol.* **1986**, *35*, 2417–2422.
[46] M. Pia Rigobello, L. Messori, G. Marcon, M. Agostina Cinellu, M. Bragadin, A. Folda, G. Scutari, A. Bindoli, *J. Inorg. Biochem.* **2004**, *98*, 1634–1641.
[47] D. M. Cheff, Q. Cheng, H. Guo, J. Travers, C. Klumpp-Thomas, M. Shen, E. S. J. Arnér, M. D. Hall, *Redox Biology* **2023**, *63*, 102719.
[48] A. Nijamudheen, A. Datta, *Chemistry A European J* **2020**, *26*, 1442–1487.
[49] B. Huang, M. Hu, F. D. Toste, *Trends Chem.* **2020**, *2*, 707–720.
[50] M. S. Messina, J. M. Stauber, M. A. Waddington, A. L. Rheingold, H. D. Maynard, A. M. Spokoyny, *J. Am. Chem. Soc.* **2018**, *140*, 7065–7069.
[51] R. Bonsignore, S. R. Thomas, M. Rigoulet, C. Jandl, A. Pöthig, D. Bourissou, G. Barone, A. Casini, *Chem. Eur. J.* **2021**, *27*, 14322–14334.
[52] R. Bonsignore, S. R. Thomas, W. T. Klooster, S. J. Coles, R. L. Jenkins, D. Bourissou, G. Barone, A. Casini, *Chemistry A European J* **2020**, *26*, 4226–4231.
[53] M. J. Frisch, G. W. Trucks, H. B. Schlegel, G. E. Scuseria, M. A. Robb, J. R. Cheeseman, G. Scalmani, V. Barone, G. A. Petersson, H. Nakatsuji, X. Li, M. Caricato, A. V. Marenich, J. Bloino, B. G. Janesko, R. Gomperts, B. Mennucci, H. P. Hratchian, J. V. Ortiz, A. F. Izmaylov, J. L. Sonnenberg, D. Williams-Young, F. Ding, F. Lipparini, F. Egidi, J. Goings, B. Peng, A. Petrone, T. Henderson, D. Ranasinghe, V. G. Zakrzewski, J. Gao, N. Rega, G. Zheng, W. Liang, M. Hada, M. Ehara, K. Toyota, R. Fukuda, J. Hasegawa, M. Ishida, T. Nakajima, Y. Honda, O. Kitao, H. Nakai, T. Vreven, K. Throssell, J. A. Montgomery, Jr., J. E. Peralta, F. Ogliaro, M. J. Bearpark, J. J. Heyd, E. N. Brothers, K. N. Kudin, V. N. Staroverov, T. A. Keith, R. Kobayashi, J. Normand, K. Raghavachari, A. P. Rendell, J. C. Burant, S. S. Iyengar, J. Tomasi, M. Cossi, J. M. Millam, M. Klene, C. Adamo, R. Cammi, J. W. Ochterski, R. L. Martin, K. Morokuma, O. Farkas, J. B. Foresman, and D. J. Fox, *Gaussian 16*, Revision C.01.
[54] P. Hohenberg, W. Kohn, *Phys. Rev.* **1964**, *136*, B864–B871.
[55] W. Kohn, L. J. Sham, *Phys. Rev.* **1965**, *140*, A1133–A1138.
[56] Y. Zhao, D. G. Truhlar, *Theor. Chem. Acc.* **2008**, *120*, 215–241.
[57] G. Scalmani, M. J. Frisch, *J. Chem. Phys.* **2010**, *132*, 114110.
[58] D. Figgen, K. A. Peterson, M. Dolg, H. Stoll, *J. Chem. Phys.* **2009**, *130*, 164108.
[59] R. Krishnan, J. S. Binkley, R. Seeger, J. A. Pople, *J. Chem. Phys.* **2008**, *72*, 650–654.
[60] H.-M. Ko, J.-R. Deng, J.-F. Cui, K. K.-Y. Kung, Y.-C. Leung, M.-K. Wong, *Bioorg. Med. Chem.* **2020**, *28*, 115375.
[61] S. M. Meier, C. Gerner, B. K. Keppler, M. A. Cinellu, A. Casini, *Inorg. Chem.* **2016**, *55*, 4248–4259.

Manuscript received: December 5, 2023
Accepted manuscript online: January 10, 2024
Version of record online: January 24, 2024